ICNAAM 2022 – 20th Intl Conf. on Numerical Analysis and Applied Mathematics
19-25 September 2022, Heraklion, Crete, Greece

A fast 6-DoF tracking method for submerged bodies: application to fish passage through a turbine

Phoevos (Foivos) Koukouvinis[1, a)] and John Anagnostopoulos[1, b)]

[1] *National Technical University of Athens, Laboratory of Hydraulic Turbomachines, Heroon Polytechniou 9, 15780 Zografou, Athens, Greece.*

[a)] fivoskoukgmail.com; [b)] Corresponding author: j.anagno@fluid.mech.ntua.gr

Abstract. Tracking rigid body motion within flows is a rather complex topic, as it involves handling of body motion, with all related boundary and mesh manipulation complexities, plus the interaction of the flow with the described object which includes additional degrees of freedom for the body motion and rotations. Whereas there are techniques that can fully couple flow and body motion, they often lead to a rather complex and cumbersome model that inherently requires a fully transient simulation and is prone to stability constraints. In the present work, an alternative method, based on a steady flow field simulation and the assumption of Bernoulli's principle around the body under consideration, can give a realistic representation of the underlying physics of body motion, at a tiny fraction of the computational effort, enabling practical simulations of fish-like models through hydraulic machinery.

INTRODUCTION

Hydropower plays an important role in global energy production; indicatively, it is estimated that hydropower [1], produces up to 17% of electricity globally, thus being the most important contribution, reaching 70% of all the renewable energy market. Hydropower can dramatically increase the market penetration of other renewables (solar or wind), if hydro-turbines are implemented as reversible devices for energy storage[2]. The installed capacity has been steadily increasing over the years[3], with projections expecting a 3% annual increase of its contribution until the year 2030, for a Net Zero Emissions scenario[4], hence any potential impact to the environment and aquatic life will be also augmented. Thus, recent interest to fish-friendly turbine designs and concepts, as manifested through projects and publications (indicatively see [2,3]), is justified.

To this purpose, designing a fish friendly turbine is a complex task, as it involves biological and fluid mechanic aspects. Indicatively, there are several factors that can potentially affect aquatic life, such as: (1) rapid variations of pressure[4], (2) excessive shear stresses[5] and (3) blade impact[5]. Several techniques have been attempted so far, including phenomenological models[6], experimental investigations[7], or numerical tracking methods[8]. Perhaps the most interesting is the aspect of numerical tracking methods, being cheaper and safer to aquatic life.

Eulerian methods consist of VOF-like techniques, where the body is advected with a conservative color function; however, it is rather challenging to maintain the material interface sharpness. Commonly, Lagrangian methods like the Discrete Particle and Discrete Element models tend to be more effective. The most accurate techniques involve tracking the actual object in a Lagrangian reference frame, with a fully two-way coupling. Effective techniques that can do that are Immersed boundaries, Cut-Cell method, Overset method, or Dynamic meshes. However, all of them are quite cumbersome and very computationally demanding; hence in the present work a fast alternative is proposed, which although sacrifices some of the accuracy, it is much more tractable for practical applications.

NUMERICAL MODEL AND ASSUMPTIONS

The developed numerical model is based on the rigid body kinematics, as described in [9,10,11], coupled with a steady flow field in a one-way manner (flow affects the body, but not vice versa). The steady flow field is obtained

by resolving momentum and continuity equations using a steady state assumption and moving reference frames. Once the flow field has converged, the main flow variables (velocities and pressure) are exported to be used subsequently for the body tracking. Flow simulations are performed using ANSYS Fluent v2021 and CFX v2021.

The body to be described is represented using a triangular tessellation, forming a surface grid. This grid can be further simplified to a set of points, each located at the barycenter of the respective triangular element, and a surface area dS, together with the local normal vector, **n**, see also FIGURE 1a. At each point of the body's surface, the nearest neighbors (cell centers) of the solved flow field are found using a *knn*-search algorithm[12]. Then, once the closest neighbors are found, the flow variables are interpolated; in the frame of the present investigation several different methods have been used, such as Inverse Distance (ID), Radial Basis Functions (RBF), Nearest Neighbor (NN), Least Squares/Linear Regression (LS) and, as a baseline, the *scatteredInterpolant* function in Matlab, using Delaunay tessellation; all aforementioned methods give similar results. Local pressure at each face element is calculated under the Bernoulli's principle, as the sum of interpolated flow pressure, p_{flow}, plus dynamic pressure due to slip velocity, p_{dyn}, (see also FIGURE 1b) i.e.:

$$p_{local} = p_{flow} + p_{dyn} \tag{1}$$

$$p_{dyn} = \frac{1}{2}\rho\left(u_{n,flow} - u_{n,surf}\right)^2 sign\left(u_{n,surf} - u_{n,flow}\right) \tag{2}$$

where: n index implies the projection on the local surface normal vector, ρ is the flow density (taken the same as water here). Also, u_{flow} implies the velocity of the interpolated flow field, whereas u_{surf} implies the velocity of the surface element, calculated by the body kinematics, as will be detailed.

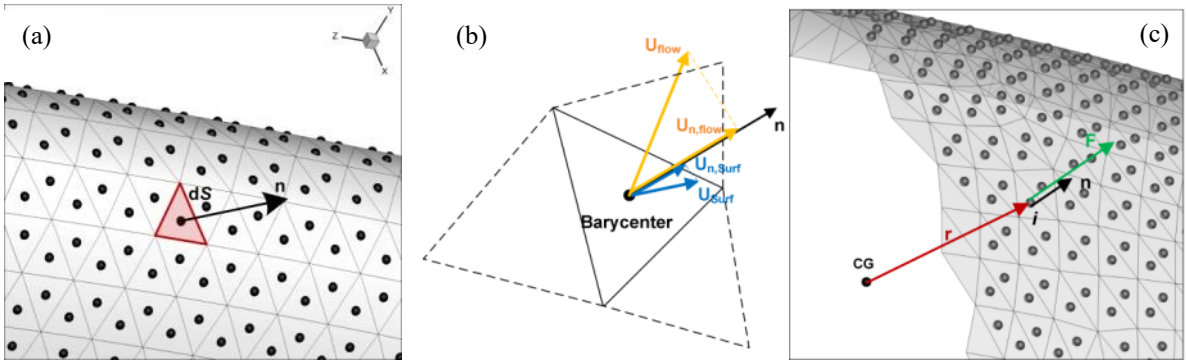

FIGURE 1. (a) Surface representation with tessellation, barycenters and normal; (b) definition of the projected slip velocity; (c) torque calculation, as the cross product of force, **F**, and distance, **r**, from the center of gravity (CG).

Once the local pressure is calculated, then the total force, **F**, and torque, **T**, on the body can be calculated by integrating the following equations along the body surface:

$$d\mathbf{F} = -p\mathbf{n}dS \tag{3}$$

$$d\mathbf{T} = \mathbf{r} \times d\mathbf{F} \tag{4}$$

where **r** is the distance of a given surface element to the center of gravity of the body, see FIGURE 1c.

Center of gravity motion can be integrated through Newton's law of motion, i.e.

$$\mathbf{F} = m\ddot{x} \tag{5}$$

where m is the body mass and $\ddot{x}$ the center of gravity (CG) acceleration. However, body rotation is more complicated, as it needs to be expressed in body-local coordinate system, where the moment of inertia tensor, I, is naturally expressed. For this, it is necessary to introduce the Euler angles, [φ, θ, ψ], which express a sequence of rotations to convert the global coordinate system to the body-local coordinate system, by first rotating around the global Z-axis (ψ), then the transformed Y-axis (θ) and finally the transformed X-axis (φ)[9]. The torques expressed in the global coordinate system are transformed to a local coordinate system, through the R transformation:

$$R = \begin{bmatrix} \cos\theta\cos\psi & \cos\theta\sin\psi & -\sin\theta \\ \sin\varphi\sin\theta\cos\psi - \cos\varphi\sin\psi & \sin\varphi\sin\theta\sin\psi + \cos\varphi\cos\psi & \sin\varphi\cos\theta \\ \cos\phi\sin\theta\cos\psi + \sin\varphi\sin\psi & \cos\phi\sin\theta\sin\psi - \sin\varphi\cos\psi & \cos\phi\cos\theta \end{bmatrix} \tag{6}$$

The transformation matrix is applied to convert global torque vector to body-local, as $\mathbf{T}_B = R \cdot \mathbf{T}_G$. Then, the body-local torque vector is used to calculate the angular acceleration at the body frame, $\dot{\boldsymbol{\omega}}_B$, keeping in mind that the body-coordinate system is rotating, hence the following formula applies:

$$\dot{\boldsymbol{\omega}}_B = I^{-1}\left(\mathbf{T}_B - \boldsymbol{\omega}_B \times I\boldsymbol{\omega}_B\right) \tag{7}$$

Then, body frame angular acceleration, can be integrated to update the body-frame angular velocities and then transformed back to the global frame, using the inverse R transformation. At the same time, angular velocities of the Euler angles, $\boldsymbol{\omega}_E$, can be calculated through the following transform:

$$\boldsymbol{\omega}_E = G\boldsymbol{\omega}_B \tag{8}$$

$$G = \begin{bmatrix} 1 & \sin\varphi\tan\theta & \cos\varphi\tan\theta \\ 0 & \cos\varphi & -\sin\varphi \\ 0 & \sin\varphi\sec\theta & \cos\varphi\sec\theta \end{bmatrix} \tag{9}$$

Integration of equations (5), (7) and Euler angles through eq. (8), is implemented using an explicit Euler, corrected Euler (Heun) or implicit Euler method[13], depending on the number of corrections applied.

FISH TRACKING IN AN AXIAL FLOW TURBINE

As an example application, in the present work, the passage of an ellipsoid object, emulating a fish, through an axial reversible hydroturbine will be examined. The turbine shown in Figure 2a was designed by previous optimization studies to be suitable for small pumped storage applications. It operates as turbine at a flow rate of 20m^3/s and head of ~12m, at 150 rpm runner speed. The ellipsoid model corresponds to the outline of a 3D CAD fish model[14] (see FIGURE 2b), with dimensions: L=0.17m, W=0.0174m , H=0.04m, mass 0.063kg, and moments of inertia I_{xx}= 1.01·10^{-4} kg.m^2, I_{yy}= 9.71·10^{-5} kg.m^2, I_{zz}=6.09·10^{-6} kg.m^2. A double scale model is also tested.

Three different sets of simulations are conducted: (1) resolving a steady-state flow field, using a moving reference frame assumption for the runner, then the flow field is used as a basis for interpolations for the simplified fish tracking approach proposed here; (2) fully coupled, transient flow field, using immersed boundaries (IB)[10]; (3) fully coupled, transient flow field, using overset meshing[11].

Results of the fish path tracking, for different fish sizes are shown in Figure 3a. When comparing with the more accurate, fully coupled body tracking methods, the fast 6DoF tracking proposed here offers a decent representation of the motion of the fish. In general, for all fish configurations tested (actual scale, double scale, zero initial velocity, zero relative initial velocity), there is a decent agreement of the fish motion. Also, the motion timings are similar between the full two-way coupling and the fast tracking approach, as can be seen in Figure 3b, where the average gauge pressure on the fish is monitored. In the same diagram, the standard deviation of this pressure is also plotted, showing satisfactory agreement regarding the magnitude, though discrepancies exist mainly in the guide vanes and rotor blades passing.

The best overall agreement is found for the smaller fish. This is justified on the main assumption of the model for small slip velocity. Other reasons for discrepancies are the full coupling used in CFX and Fluent rigid body solvers, and the strong variations of the flow field and vortex generation, due to the inherently transient approach in the fully coupled cases. Nevertheless, it should be highlighted that the fast tracking approach proposed here requires about two orders of magnitude less computational time than the full coupling techniques.

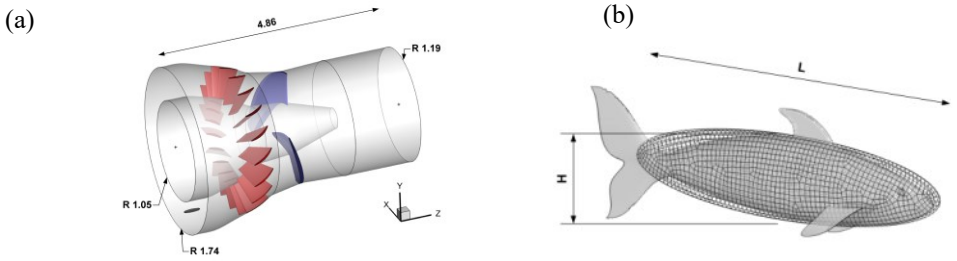

FIGURE 2. (a) Geometry of the reversible axial turbine tested; the stator is shown with red, rotor blades are blue. Dimensions in *m*. (b) The ellipsoid used to emulate the fish geometry.

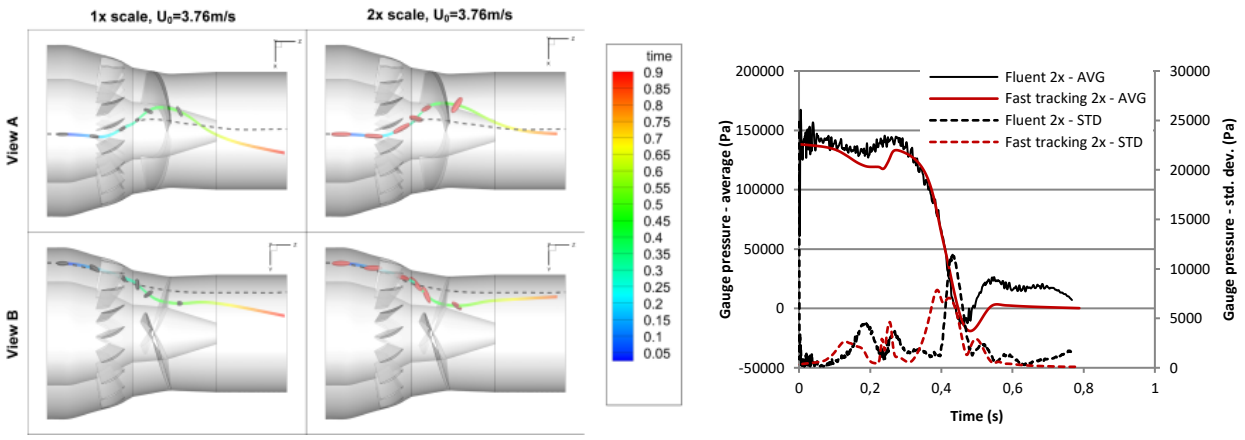

(a) (b)

FIGURE 3. (a) Indicative instances of the body motion for normal and double scale fish. Ellipses are body instances from the Fast tracking simulation at (from left to right) 5ms, 165ms, 267ms, 329ms, 391ms, 495ms. The colored line is the trace of the body path; Dashed lines: streamlines. (b) pressure distribution statistics over the moving body for double scale.

CONCLUSION

A fast fish-tracking algorithm is presented in the present work, which can be a valuable tool for estimating safe fish passage through modern turbine concepts. The algorithm relies on several simplifications, such as the assumption of Bernoulli's principle around the fish and the use of a steady-state flow field, however it can predict a motion path similar to fully coupled solvers, at a tiny fraction of the computational cost (several days on parallel workstation, vs less than an hour as a single core process). Thus, the fast tracking approach can be used for extensive analysis and derivation of statistics regarding the various interactions of fish passing through hydroturbines.

ACKNOWLEDGMENTS

This research has been co-financed by the European Union and Greek national funds through the Operational Program Competitiveness. Entrepreneurship and Innovation, under the call RESEARCH–CREATE–INNOVATE (project code: T1EDK-01334, 2018–2023).

REFERENCES

1. Å. Killingtveit, *15 - Hydroelectric Power* (Elsevier Ltd, 2020).
2. R. Van Treeck, J. Radinger, N. Smialek, J. Pander, J. Geist, M. Mueller, and C. Wolter, Sustain. Energy Technol. Assessments **51**, 101906 (2022).
3. R. Kumar, A. Abbas, G. Dwivedi, and S.K. Singal, Mater. Today Proc. (2020).
4. R.S. Brown, B.D. Pflugrath, A.H. Colotelo, C.J. Brauner, T.J. Carlson, Z.D. Deng, and A.G. Seaburg, Fish. Res. **121**–**122**, 43 (2012).
5. C.H.C.C. Outant, 351 (2000).
6. B.P.M. van Esch and I.L.Y. Spierts, Can. J. Fish. Aquat. Sci. **71**, 1910 (2014).
7. T. Fu, Z.D. Deng, J.P. Duncan, D. Zhou, T.J. Carlson, G.E. Johnson, and H. Hou, Renew. Energy **99**, 1244 (2016).
8. M.C. Richmond and P. Romero-Gomez, IOP Conf. Ser. Earth Environ. Sci. **22**, 62010 (2014).
9. B. Etkin, *Dynamics of Atmospheric Flight* (Dover Publications, 2005).
10. ANSYS, in *ANSYS V2021, CFX Theory Guid.* (n.d.).
11. ANSYS, in *ANSYS Fluent V2021, User Man.* (n.d.).
12. J.H. Friedman, J.L. Bentley, and R.A. Finkel, ACM Trans. Math. Softw. **3**, 209 (1977).
13. E. Süli and D.F. Mayers, *An Introduction to Numerical Analysis* (Cambridge University Press, 2003).
14. R. Ozdemir, Fish surface loft,https://grabcad.com/library/fish-surface-loft.